
Topology optimization for additive manufacturing

Kazybek Kassym¹, Konstantinos Kostas¹, Didier Talamona¹

Nazarbayev University, MAE – School of Engineering and Digital Sciences, Nur-Sultan, Kazakhstan¹

Corresponding author: didier.talamona@nu.edu.kz

Abstract

The main aim of this project is to assess the use of topology optimization (TO) methods in additive manufacturing in conjunction with the effect of 3D-printing parameters on the resulting strength of the printed parts. The two most common topology optimization methods, i.e., Density-based and Level-Set methods, were used with the aim of minimizing the mass of a given prototype solid entity while maintaining, to the extent possible, its tensile strength. A family of designs was produced for different levels of retained mass. Specifically, topologically optimized designs were generated for mass levels ranging from 50% to 100% of the original entity's mass with a 10% step. These designs were experimentally assessed in conjunction with varying infill patterns and infill density parameters of the employed Fused Deposition Modeling (FDM) printer (Ultimaker S3). The assessment was carried out systematically via tensile testing of the 126 printed specimens (using at least 3 samples for each model) and generation of the corresponding stress-strain graphs. In summary, the non-optimized entities and the 10%-mass-reduced designs exhibited practically identical strengths, whereas the 30% and 50%-mass-reduced ones exhibited slightly lower values for the maximum load at specimen's failure. The general trend of maximum stress was almost the same with slight deviations in average values, while standard deviation for some of the models was high. Furthermore, the employed density-based TO method appeared to produce parts that are better suited for 3D printing as it was computationally inexpensive, and it consistently generated designs that outperformed the ones generated by the Level-Set method. Regarding 3D-printing parameters, it was observed that the 'triangle', 'line' and 'grid' patterns produce printouts with practically equivalent strength. Finally, for parts produced with low values of infill density unexpected results and break points were observed. This can be explained by the introduction of large gaps in the interior of the printed model that negatively affect the strength of the part. Further investigation is needed to assess, qualitatively and quantitatively, the effect of infill density on the strength of printed parts.

Keywords: Optimization, Design method, Algorithm, Additive Manufacturing

1. Introduction

The current development of additive manufacturing has contributed to increased production of complex mechanical parts with minimum material waste [1, 2]. At the same time manufacturers are implementing additive manufacturing approaches with the aim of producing complex shapes that can reduce the weight of products and/or components of interest without compromising their mechanical properties [3]. Topology optimization in this context is commonly implemented via appropriate methods (and corresponding software packages) that modify the component's material distribution by mainly removing material from the considered solid entity [4-5]. The modified topological structure, within the constrained design space determined by the application, will make the optimized component lighter while ideally maintaining the same strength. Obviously, additional performance criteria may be used and therefore the topology optimization result will generally satisfy the design constraints of the initial design and at the same time provide identical performance with reduced weight.

The most popular approaches used in relevant industries are Solid Isotropic Material with Penalization (SIMP) and Level-Set topology optimization methods [6]. The SIMP or Density-based approach performs optimization via a voxelization approach that is commonly computationally inexpensive. The approach results in a material density scalar field considering the corresponding

Young's modulus. The value of the penalty factor manipulates the addition of elements with intermediate densities to the total stiffness. Numerical experiments show that the penalty factor that is equal to 3 is the most suitable. [7]. The Level-Set Method (LSM) for topology optimization uses iso-contours of Level-set function to implicitly determine the interfaces between entity boundaries [8]. This approach, contrary to most density-based approaches, allows boundaries to be smoothly defined.

2. Methodology

Our approach in this work consists of the following major steps: static structural setup for each model instance, topology optimization, 3d printing of resulting optimized component (3 identical components printed for each case), tensile testing and extraction of load-elongation graph and analysis of the results. The details of each step are described in the following sections.

2.1. Static Structural Setup

Firstly, the geometry of the employed object should be determined and designed for further processing. There are essential conditions that our model needs to satisfy, e.g., the dimensions of the specimen should fit into the tensile test machine which has a maximum width of 25mm.

After reviewing pertinent publications [15,18,23] which included tensile tests on 3D printed plastic materials, the model shown in Figure 1 has been selected. The design of the model is

symmetric with respect to two planes (x-y and y-z; see Fig. 1). The geometry of the model is split into three parts, two side parts of identical shape and the middle part which is a quadrangular prism. Smooth transitions have been created between these parts to avoid stress concentrations. The model was drawn in SpaceClaim¹ software for further static structural analysis in Ansys².

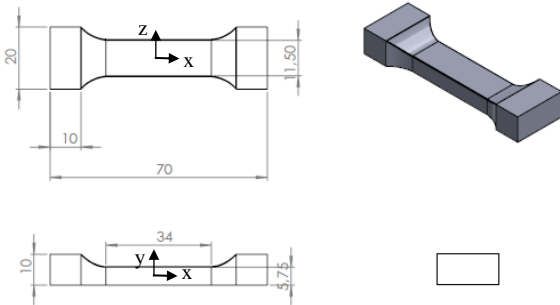


Figure 1. Sketch of the model

The two main modules for performing topology optimization in ANSYS Workbench are Static Structural and Topology Optimization [16]; see also Fig 2. Firstly, it is necessary to draw or import the geometry of the object into Static Structural, where the initial setup and meshing take place. To perform numerical solution of maximum stress, elongation at break or rigidity, the static structural analysis within the corresponding ANSYS workbench should be carried out. In Fig. 3 we see that one boundary face was selected for applying fixed support while the opposite face is subject to a normal force (100N) pulling the specimen. This is done to calculate the equivalent stress distribution along the model during the tensile test. After completion of structural analysis, all relevant information (engineering data, geometry, model setup, and solution) are transferred to the topology optimization module. In this module, we configure the optimization problem by specifying the objective function, optimization constraints, satisfaction tolerances, max iterations, percent of retain and other relevant algorithmic parameters. The module offers various topology optimization algorithms including the ones we have identified, i.e., density based and level-set methods [16]. In both cases, at each iteration of the topology optimization algorithm, the modified geometry is transferred again to a new Static Structural module, for analysis of its new structural characteristics. The second structural module is linked to the initial one and retrieves all relevant information, as needed, for analysis [17].

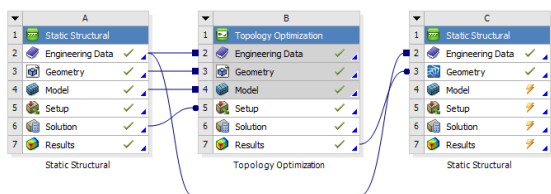


Figure 2. The Ansys modules connection

2.2. Mesh refinement and convergence

To produce accurate results, it is necessary to refine and optimize the mesh of the selected geometry. Identifying the optimum element and mesh sizes saves processing time while producing highly quality outcomes. Initially, the default ANSYS mesh settings were used followed by refinement and adjustments needed for sensitivity analysis and mesh convergence.

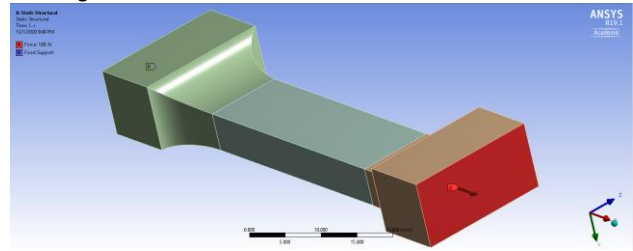


Figure 3. Model in Ansys

The maximum equivalent stress has been selected for checking the mesh quality of the model. ANSYS has a built-in mesh convergence tool, that was used in this work. The maximum level of mesh refinement was set to 5 with each level generating a finer mesh when compared to the previous one. Mesh converges when the change of RMS error of equivalent stress is less than 1%. Table 1 shows mesh refinement results for 3 different meshes that were produced by the mesh convergence tool. The initial mesh has 25985 nodes, 10659 elements and has an element size (maximum edge size) of 1mm with the maximum equivalent stress of 7.68 MPa, while the second mesh has significantly more nodes and elements resulting in an equivalent stress value of 7.82 MPa. The RMS error for the equivalent stress, calculated between the first two meshes, was slightly above 2.3%. However, the RMS error between the second and third mesh went down to 0.16%, which is below the set threshold. Hence, convergence stops at the third iteration, and this third mesh with 640581 nodes, 263626 elements and an element size of approximately 0.3 mm is used in analysis; see also Fig. 4.

Table 1 Mesh refinement results (Ansys generated table)

	Equivalent stress (MPa)	Change, %	Nodes	Elements
1	7.6853		25985	10659
2	7.8295	2.324812	278424	112851
3	7.8305	0.161422	640581	263626

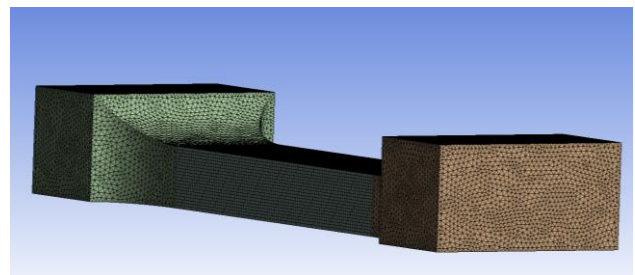


Figure 4. The final mesh of the model with 0.3mm element size

Figure 5 shows the distribution of equivalent stress during pull. Red regions correspond to higher values of stress and blue hues correspond to regions with low stress values. It can be clearly seen that comparatively high stress values are exhibited at the middle region.

¹ "SpaceClaim is a solid modeling CAD software developed by SpaceClaim Corporation."

² "Ansys engineering simulation and 3D design software delivers product modeling solutions with unmatched scalability and a comprehensive Multiphysics."

As mentioned previously, to efficiently perform topology optimization, the model was split into three parts with the middle part being the only part considered for design optimization [19]. Theoretically, the model is expected to break, during tensile testing, at the middle since the cross section there is thinner [18].

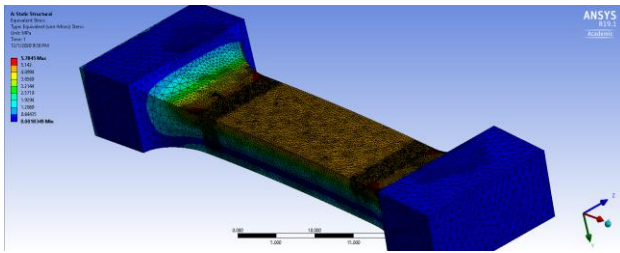


Figure 5. Distribution of equivalent stresses

Tables 2 and 3 record the volumes/material mass for the complete body and the middle part after optimization for various levels of material reduction. The difference between the two tables relates to the different infill density values. Specifically, Table 2 corresponds to an infill density of 100% that produces savings between 2.9% and 14.6%, whereas for the 60% infill density case (Table 3) savings go up to 50%.

Table 2 The volume of the model and reduction percent using 100% infill density.

Percent of retain, %	Volume of middle body, cm ³	Total volume, cm ³	Material reduction of middle body, g
100	2,25	7,70	0
90	2,02	7,47	0,55
80	1,80	7,25	1,11
70	1,57	7,02	1,67
60	1,35	6,80	2,22
50	1,12	6,57	2,78

Table 3 The volume of the model and material reduction percent using 60% infill density

Percent of retain, %	Volume of optimized body, cm ³	Total volume, cm ³	Material reduction of middle body, g
100	2,25	4,62	0,33
90	2,02	4,48	0,666
80	1,80	4,35	1,002
70	1,57	4,21	1,332
60	1,35	4,08	1,668
50	1,12	3,94	0,33

The topology optimization setup is shown in Fig. 6 which presents analysis and corresponding constraint settings. The convergence accuracy is set to be 0.1% while the maximum number of iterations is equal to 500 by default. The 'response constraint' category has an adjustable parameter corresponding to the "percent of retain" that needs to be preserved. Topology optimization in Ansys can be performed with respect to mass, volume, center of gravity, moment of inertia, global/local von-Mises stress, displacement, reaction force, compliance, and many others [19]. The results presented in this work correspond to mass usage optimization.

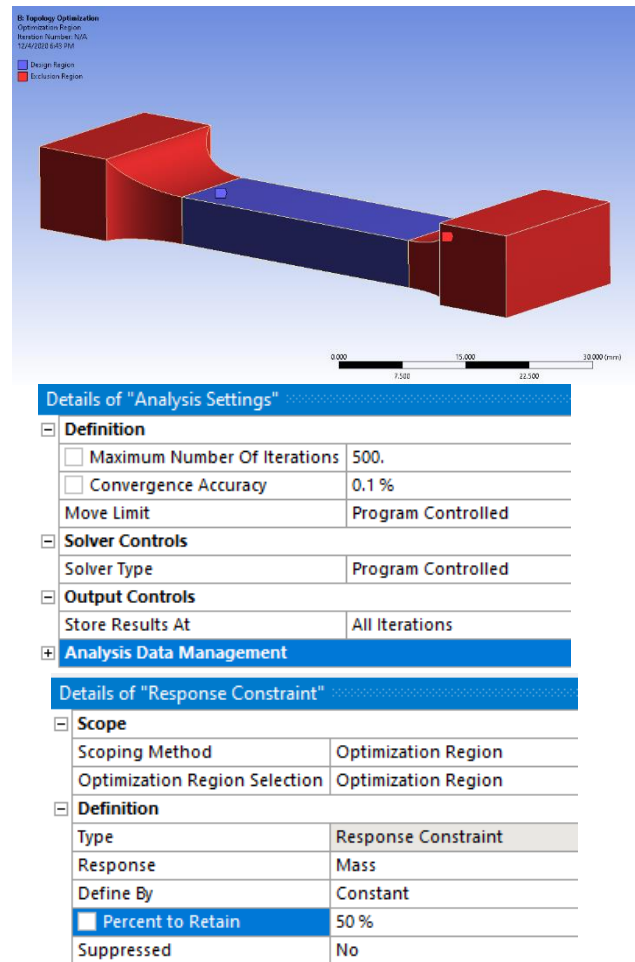


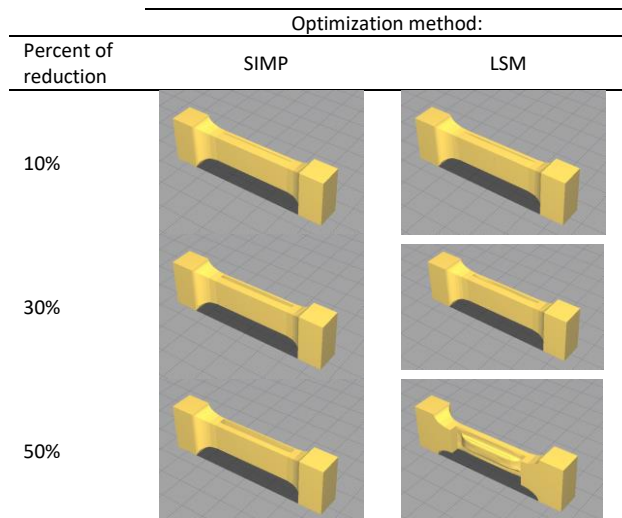
Figure 6. Region optimization and setup

3. Results

Tables 4 and 5 record the optimized designs for percent of retain. The resulting designs of the middle body part use less material in regions where stress concentration was low for both methods. The two methods exhibit variations for the cases of 90% and 50% of retain, while 70% of retain has almost similar results for both of them.

Table 4 Optimized body of the specimen

Optimization type: →	SIMP	LSM
Percent of retain: ↓		
90%		
70%		
50%		

Table 5 Structurally evolved design of the specimen

The next step consists of manufacturing the optimized models using a FDM 3D-printer and test them in tension to failure. A speed rate of 5mm/min was used, based on pertinent literature. Table 6 contains tensile test results for SIMP-optimized specimens with triangular infill pattern, 100% infill density and 50%, 70% and 90% of retain. By averaging the load at break for the three specimens it can be seen that a 10% reduction of weight with TO results in an increase of load capacity per unit area of 5%, a small reduction of 1% for 30% and an increase of 8% for 50%.

Table 6 SIMP, 100% infill, triangle

Specimen #	Percent of retain	Optimization time, min	Printing time, min	Max stress, MPa	Yield stress, MPa	Young's M, MPa	Elong. at break, mm	Load at break point, N
1	50%	11	152	52,75	52,70	1687	2,50	1654
2	50%	11	152	49,81	49,80	2119	2,23	1548
3	50%	11	152	49,03	49,00	2556	1,66	1621
4	70%	10	163	53,38	53,38	2055	1,98	2471
5	70%	10	163	49,46	49,42	2214	1,79	1964
6	70%	10	163	41,07	41,07	2244	1,57	1740
7	90%	15	171	45,54	45,51	1742	2,07	2710
8	90%	15	171	41,55	41,53	1649	2,01	2473
9	90%	15	171	54,26	54,25	1417	2,66	3229
10	100%	0	146	44,91	44,91	1785	2,21	2969
11	100%	0	146	45,61	45,61	1668	2,30	3016
12	100%	0	146	43,98	43,95	1661	2,20	2908

4. Conclusion

In conclusion, topology optimization of simple 3D model has been successfully performed with interesting results. An initial investigation of printing parameters, such infill pattern shape and density, has been also performed. From tensile testing results, we observe that a slight increase of load carrying capacity per unit area can be achieved. At the same time, we have observed failures for some topologically optimized specimens that can be attributed to several reasons, including stress concentrations at abrupt cross-section changes, gaps introduced by low infill density along with the position the starting/ending deposition point of each printed layer that generates weak points. Further investigation is needed to such cases.

Acknowledgement:

This research was funded by Nazarbayev University under the Faculty Development Competitive Research Grant Program No 240919FD3923, "Cost effective hybrid casting methods for cellular structures".

References

- [1] Ngo, T.D., Kashani, A., Imbalzano, G., Nguyen, K.T. and Hui, D., 2018. Additive manufacturing (3D printing): A review of materials, methods, applications and challenges. *Composites Part B: Engineering*, 143, pp.172-196.
- [2] Clausen, A., 2016. Topology optimization for additive manufacturing. *DTU Mechanical Engineering*.
- [3] Ranjan, R., Samant, R. and Anand, S., 2017. Integration of design for manufacturing methods with topology optimization in additive manufacturing. *Journal of Manufacturing Science and Engineering*, 139(6).
- [4] Pedersen, C.B. and Allinger, P., 2006. Industrial implementation and applications of topology optimization and future needs. In *IUTAM Symposium on Topological Design Optimization of Structures, Machines and Materials* (pp. 229-238). Springer, Dordrecht.
- [5] Saadlaoui, Y., Milan, J.L., Rossi, J.M. and Chabrand, P., 2017. Topology optimization and additive manufacturing: Comparison of conception methods using industrial codes. *Journal of Manufacturing Systems*, 43, pp.178-186.
- [6] Kentli, A., 2020. Topology optimization applications on engineering structures. *Truss and Frames—Recent Advances and New Perspectives*, pp.1-23.
- [7] Erdelyi, H., Herz, M., Lemaire, E., Paffrath, M. and Wever, U., *Aspects of Industrial Topology Optimization*.
- [8] Sethian, J.A. and Wiegmann, A., 2000. Structural boundary design via level set and immersed interface methods. *Journal of computational physics*, 163(2), pp.489-528.
- [9] Liu, J., Gaynor, A.T., Chen, S., Kang, Z., Suresh, K., Takezawa, A., Li, L., Kato, J., Tang, J., Wang, C.C. and Cheng, L., 2018. Current and future trends in topology optimization for additive manufacturing. *Structural and Multidisciplinary Optimization*, 57(6), pp.2457-2483.
- [10] Langelaar, M., 2017. An additive manufacturing filter for topology optimization of print-ready designs. *Structural and multidisciplinary optimization*, 55(3), pp.871-883.
- [11] Stavropoulos, P. and Foteinopoulos, P., 2018. Modelling of additive manufacturing processes: a review and classification. *Manufacturing Review*, 5, p.2.
- [12] Li, N., Huang, S., Zhang, G., Qin, R., Liu, W., Xiong, H., Shi, G. and Blackburn, J., 2019. Progress in additive manufacturing on new materials: A review. *Journal of Materials Science & Technology*, 35(2), pp.242-269.
- [13] Grinde, S., 2018. Topology Optimization for Additive Manufacturing Using SIMP Method.
- [14] Peirce, C.S. and De Waal, C., 2014. *Illustrations of the Logic of Science*.
- [15] Beshimbay, D. and Kereyeva, A., 2018. 3D-PLA-plastics.
- [16] Lee, H.H., 2018. Finite element simulations with ANSYS Workbench 18. SDC publications.
- [17] Thompson, M.K. and Thompson, J.M., 2017. ANSYS mechanical APDL for finite element analysis. Butterworth-Heinemann.
- [18] Hosford, W.F., 1992. Overview of tensile testing. *ASM International, Tensile Testing (USA)*, 1992, pp.1-24.
- [19] Li, X.P., Zhao, L.Y. and Liu, Z.Z., 2017. Topological optimization of continuum structure based on ANSYS. In *MATEC Web of Conferences* (Vol. 95, p. 07020). EDP Sciences.